Atmos. Chem. Phys. Discuss., 9, 20229–20257, 2009
www.atmos-chem-phys-discuss.net/9/20229/2009/


**Atmospheric Chemistry and Physics Discussions**

This discussion paper is/has been under review for the journal *Atmospheric Chemistry and Physics (ACP)*. Please refer to the corresponding final paper in *ACP* if available.

# On retrieval of lidar extinction profiles using Two-Stream and Raman techniques

**I. S. Stachlewska**[1,2] **and C. Ritter**[1]

[1]Alfred Wegener Institute for Polar and Marine Research, Telegrafenberg A43, 14473 Potsdam, Germany
[2]Institute of Geophysics, Faculty of Physics, University of Warsaw, Pasteura 7, 02-093 Warsaw, Poland

Received: 8 July 2009 – Accepted: 14 September 2009 – Published: 28 September 2009

Correspondence to: I. S. Stachlewska (iwona.stachlewska@igf.fuw.edu.pl)

Published by Copernicus Publications on behalf of the European Geosciences Union.



**Abstract**

The Two-Stream technique employes simultaneous measurements performed by two elastic backscatter lidars aiming at each other to sample into the same atmosphere. It allows for a direct retrieval of the extinction coefficient profile from the ratio of the two involved lidar signals. During a few Alfred-Wegener-Institute's (AWI) campaigns dedicated to the Arctic research, the AWI's Polar 2 aircraft with the integrated on-board nadir-aiming Airborne Mobile Merosol Lidar (AMALi) overflew a vicinity of Ny Ålesund on Svalbard, where the zenith-aiming Koldewey Aerosol Raman Lidar (KARL) has been located. This experimental approach gave a unique opportunity to retrieve the extinction profiles with rather rarely used Two-Stream technique against the well established Raman technique. Both methods were applied to data obtained for a clean Arctic conditions during the Arctic Study of Tropospheric clouds and Radiation (ASTAR 2004) campaign and a slightly polluted Arctic conditions during the Svalbard Experiment (SvalEx 2005) campaign. Successful intercomparison of both evaluation tools in a different measurement conditions demonstrates sensitivity and feasibility of the Two-Stream method to obtain particle extinction and backscatter coefficients profiles without assumption of their relationship (lidar ratio). The method has a potential to serve as an extinction retrieval tool for KARL or AMALi simultaneous observations with the spaceborne CALYPSO lidar taken during the ASTAR 2007.

## 1 Introduction

Retrieval of the particle microphysical parameters (particle effective radius, index of refraction and size distribution), from lidar derived optical properties of particles in the atmosphere (particle extinction and backscatter coefficient profiles) consists of a mathematically ill-posed inversion problem (Böckmann, 2001). The emergent efficiencies, typically taken from Mie theory, act differently for extinction and backscatter coefficient. Hence, any inversion of microphysical parameters feeded with both coefficients cal-

culated independently is performed more precisely, especially for the determination of the particle size distribution (Müller et al., 1999; Veselovskii et al., 2002; Böckmann and Kirsche, 2006). Obtaining information on the particle extinction $\alpha^{\text{part}}(h)$ and backscatter $\beta^{\text{part}}(h)$ coefficients without often used assumption of their relationship signifies a great step forward into interpretation of lidar data. Unfortunately, the comonly used elastic backscatter lidar cannot alone provide a complete information for the inversion of the microphysical parameters (two unknown coefficients in one equation describing a lidar return signal, Eq. 1). The standard Klett-Fernald-Sasano approach for the evaluation of elastic backscatter lidar data (Klett, 1981; Fernald, 1984; Klett, 1985; Sasano, 1985) requires knowledge or assumption of the backscatter coefficient calibration value $\beta_{\text{ref}}$ and the lidar ratio $B(h)=\frac{\alpha^{\text{part}}(h)}{\beta^{\text{part}}(h)}$. The latter one is usually a not very well known atmospheric property, as it greatly varies with the chemical composition and size distribution of the aerosol particles present in the atmosphere (Ackermann, 1998).

If the elastic backscatter lidar is additionaly equipped with the Raman-shifted detection channels an independently obtained extinction profile can be contributed towards analytical solution for the retrieval (Ansmann et al., 1990, 1992). The cross-section for the inelastic Raman scattering of the laser light with matter is almost three orders of magnitude lower than the cross-section for the elastic Rayleigh/Mie scattering. This results in significantly noise polluted signals obtained from the Raman channels. The Raman signals are usualy strongly averaged in time and range for the further analyses, which can severly influence the results of the Raman extinction coefficient retrieval (Pornsawad, 2008).

There is another, rather raerly applied, approach which provides an independent information into the classic solution of the lidar problem. The Two-Stream inversion, also referred to as the bipath or the double-ended lidar technique, requires two elastic backscatter lidars aiming at each other. The method was introduced already in th 80ties (Kunz, 1987; Hughes and Paulson, 1988), revised for an application to ground-based lidars horizontaly aiming at each other (Jörgensen et al., 1997), applied to zenith-aiming ground-based lidar and nadir-aiming airborne lidar experimental data (Stachlewska et



al., 2005; Ritter et al., 2006), and finally, discussed for zenith-aiming ground-based lidar and nadir-aiming spaceborne lidar (Cuesta and Flamant, 2004; Wang et al., 2007). The Two-Stream technique allows a direct retrieval of height dependent extinction coefficient with the only assumption that the atmosphere sampled from the opposite directions by the two lidars is the same. With this method also the backscatter coefficient can be obtained directly, if any of the employed lidar instrumental constants $C$ or a backscatter reference value $\beta_{\text{ref}}$ at any given height in the interval covered by lidars' simultaneous observations are known.

In this paper we present, a study dedicated to the direct comparison of the Two-Stream particle extinction and backscatter coefficient profiles and the lidar ratio profiles with the respective Raman retrievals.

The Two-Stream method was applied to data recorded during simultaneous measurements taken with the nadir-aiming Airborne Mobile Aerosol Lidar (AMALi), integrated onboard the AWI research aircraft Polar 2, overflying the zenith-aiming Koldewey Aerosol Raman Lidar (KARL) based in Ny Ålesund on Svalbard. Both lidars and their configuration during the measurements are shortly discussed in the Appendices A and B. The Two-Stream $\beta^{\text{part}}_{\text{TS}}(h)$, $\alpha^{\text{part}}_{\text{TS}}(h)$ and $B_{\text{TS}}(h)$ profiles obtained on 15 May 2004 and 19 May 2004 during the the Arctic Study of Tropospheric clouds and Radiation (ASTAR) campaign and on 14 April 2005 during the Svalbard Experiment (SvalEx) campaign are discussed in this paper. On each of these days the KARL performed the Raman and elastic backscatter measurements for which the Raman $\alpha^{\text{part}}_{\text{RM}}(h)$ and $\beta^{\text{part}}_{\text{RM}}(h)$ and $B_{\text{RM}}(h)$ were retrived. Good agreement of the results obtained with the two evaluation techniques proves the feasibility of the two stream methodology for the application to the nadir-aiming, low altitude, airborne lidar measurements.

In the future we will evaluate the data collected during the ASTAR 2007 by the zenith-aiming airborne AMALi and the satellite CALYPSO lidar (Winker et al., 2007) to perform a feasibility study of this configuration.

## 2 Theoretical background

In our case the measuring scheme consists of a zenith-aiming ground based lidar (denoted $K$) and overflying it at a height $h_f$ nadir-aiming airborne lidar (denoted $A$). Assuming that the same air is probed when the airborne lidar overflies the ground based lidar, both systems perceive this same air differently; the ground based system with density decreasing with height and vice versa for the airborne instrument. This ensures mathematically independent information content in both lidar equations.

The elastic lidar equation describes the received signal as a function of the atmospheric and system parameters, whereby assumptions of quasi-monochromatic coherent emitted laser light and instantaneous elastic or inelastic scattering are taken into account, while processes of multiple scattering of light are being neglected (Kovalev and Eichinger, 2004). The lidar equation is usually used in a form of the range corrected signal $S(h)$, obtained by multiplication of the detected signal with the squared range vector. The ground based lidar equation can be written as in Eq. (1) and airborne lidar equations as in Eq. (2).

$$S_K(h) = P_K(h)h^2 = C_K\beta(h)T^2_{[0,h]}(h) \tag{1}$$

$$S_A(h) = P_A(h)(h_f - h)^2 = C_A\beta(h)T^2_{[h_f,h]}(h) \tag{2}$$

The $h$ denotes the distance between lidar and target particles or molecules, the $P(h)$ intensity of the detected backscattered signal at a time $t=2h/c$, the $C$ lidar instrumental constant, and the $\beta(h)=\beta^{\mathrm{mol}}(h)+\beta^{\mathrm{part}}(h)$ is the total backscatter coefficient, due to molecules and particles present at the height $h$. The last term $T$ describes the atmospheric transmittance (Eq. 3) between the ground based or airborne lidar and the height $h$.

$$T(h,\lambda) = \exp\left(-\int_{h_0}^{h}\alpha\left(\tilde{h},\lambda\right)d\tilde{h}\right) \tag{3}$$



The $\alpha_{\mathrm{TS}}(h)=\alpha^{\mathrm{mol}}_{\mathrm{scat}}(h)+\alpha^{\mathrm{part}}_{\mathrm{scat}}(h)+\alpha^{\mathrm{mol}}_{\mathrm{abs}}(h)+\alpha^{\mathrm{part}}_{\mathrm{abs}}(h)$ is the total extinction coefficients depending on the total number of molecules and particles scattering and/or absorbing the laser light at the height $h$.

In the Two-Stream approach we are dealing with the simultaneous equation system which has four unknowns (two unknown lidar instrumental constants $C_K$ and $C_A$ and unknown $\alpha$ and $\beta$ coefficients). By dividing Eq. (2) by Eq. (1) the backscatter coefficients terms are eliminated and an expression for the height dependent extinction coefficient can be obtained (Eq. 4). Obtained this way $\alpha_{\mathrm{TS}}(h)$ does not require any a priori assumption or further calibration and normalisation.

$$\alpha_{\mathrm{TS}}(h) = \frac{1}{4}\cdot\frac{d}{d\,h}\left(\ln\left(\frac{S_A(h)}{S_K(h)}\right)\right) \tag{4}$$

Note that after the successful retrieval of the extinction coefficient the atmospheric transmittance can be obtained, and, hence, the ratio between both lidar instrumental constants $\frac{C_A}{C_K}$ is known by division of Eq. (2) by Eq. (1). The $C_A$ and $C_K$ can be estimated directly from the Eqs. (1) and (2) if at any height within the Two-Stream application range there is avaliable additional information on $\beta_{\mathrm{ref}}$ (known for aerosol free range in the hight Troposphere) or the lidar $B(h)$ (known $B_{\mathrm{Ci}}$ for Cirrus clouds).

An assumption, that exactly the same air parcels are probed by both lidars during overflights implies, that there exists only one representative profile of $\alpha(h)$ and $\beta(h)$ for the sampled air. Therefore the knowledge of any of the lidar instrumental constants $C_K$ or $C_A$ allows for a direct calculation of the backscatter profile from Eqs. (1) or (2), respectively. Alternatively, the backscatter profiles can be derived from the Two-Stream approach by multiplying Eq. (1) by Eq. (2).

## 3 Experimental results

The applicability of the Two-Stream method depends critically on the constraint that both lidars probe into the same air masses. The best matching periods for the over-

flights were found by correlating the measured signals (Ritter et al., 2006). This was done by constructing a correlation map between both lidars' data sets corresponding to the time of the overflight. For all data sets at times $t_i$, $t_j$ the correlation coefficient was calculated accordingly to Eq. (5) in which extinction cefficient was obtained with assumption of a constant lidar ratio ($B$=30) using standard Klett-Fernald-Sasano inversion.

$$CC_{i,j} := \mathrm{corr}\left\langle S_A(h,t_i)\cdot\exp\left(+2\int\alpha(h)\right), S_K(h,t_j)\cdot\exp\left(-2\int\alpha(h)\right)\right\rangle \quad (5)$$

The choice of $B$ influenced the values of the correlation coefficients but it did not have an effect on their relative minima and maxima. Moreover, if one lidar recorded clouds or aerosol layers at another altitude than the other lidar (typical situation near the coastline) it was easily detected as a shift in the data sets.

For all days under consideration the data sets at times providing the absolute maximum of the correlation coefficient have been selected for the evaluation. As a result more range than required by constraints of each lidar's geometrical compression was excluded for calculation (different air masses directly above the station and directly below the aircraft due to the aircraft's flightpath).

Both data sets were averaged over 60 m in altitude. Shortest possible temporal averaging providing sufficient SNR was applied: 10 min for the ground-based system and 8 min for the airborne lidar. The $\alpha_{\mathrm{TS}}(h)$ profiles were derived directly from Eq. (4) without any noise-treatment, as the extinction coefficient retrieval is methematically an ill-posed problem and even slight noise filtering can sevearly influence the inversion result (Pornsawad, 2008). Smoothing was applied only to already calculated $\alpha_{\mathrm{TS}}(h)$ by a running mean of 300 m.

The Rayleigh extinction $\alpha^{\mathrm{mol}}(h)$ and backscatter $\beta^{\mathrm{mol}}(h)$ profiles due to the existence of the molecules in the probed atmosphere were calculated from temperature and pressure profiles measured by daily radiosonde launches at the Koldewey Station in Ny Ålesund. These were substracted (Rayleigh calibration) from the total $\alpha(h)$ and $\beta(h)$ profiles to obtain the particle $\alpha^{\mathrm{part}}(h)$ and $\beta^{\mathrm{part}}(h)$ profiles. The same substraction



procedure was applied for the two-stream, the Raman, and the Klett-Fernald-Sasano approach.

The absorption contribution at 532 nm (mostly due to ozone) is negligible in the Arctic troposphere and thus was not considered in this analysis.

The particle optical depth calculated with the Two-Stream approach, i.e. $\tau_{\mathrm{TS}}^{\mathrm{part}}$, was obtained by integration of the $\alpha_{\mathrm{TS}}^{\mathrm{part}}$ profiles over the range interval avaliable for the Two-Stream application, which was estimated using the correlation algorithm applied prior to the evaluation (Eq. 5).

Information on the particle optical depth of the whole atmosphere $\tau_{\mathrm{sun}}^{\mathrm{part}}$ was obtained from almost simultaneous measurements using the multi-channel Spectrophotometer SP1A-14 (Dr. Schulz & Partner, Buckow, Germany). Instrument's measuring range covers UV, VIS and IR light spectrum, where 8 channels are selected accordingly to the WMO/1983 recommendation and VDI 3786/10/3/ recommendation (368, 412, 500, 600, 675, 778, 862, 1024 nm) and 10 are additional (353, 389, 450, 532, 760, 911, 946, 967, 1045, 1064 nm). A full measuring cycle, i.e. collecting and storing the data of 18 channels and calling up the next cycle, is taken within 8 s. Calibration is performed with artifical radiation sources at the optical laboratory using the Leiterer calibrating method Leiterer et al. (1985) or during a field experiment using the Langley-extrapolation method. The latter one must be performed in a case of cloud absence along the optical path and extremely low variations in the planetary boundary layer, conditions often occuring under a very clear air conditions in the polar regions. For the analyses discussed in this paper we used the spectrophotometer measurements taken at the 532 nm channel.

For intercomparisons the particle optical depth obtained within the avaliable Two-Stream range $\tau_{\mathrm{TS}}^{\mathrm{part}}$ (lower troposphere), the sunphotometer's particle optical depth $\tau_{\mathrm{sun}}^{\mathrm{part}}$ (whole atmosphere), and the tropospheric particle optical depth $\tau_{\mathrm{KFS}}^{\mathrm{part}}$ (almost whole troposphere) was integrated from $\alpha_{\mathrm{KFS}}^{\mathrm{part}}$ over avaliable range of the KARL's standard elastic Klett-Fernald-Sasano retrieval.

Note that we took the lowest $\tau_{\text{sun}}^{\text{part}}$ value (corresponding to the highest Ångstrøm exponent) for times with the lowest Cirrus contamination in the upper troposphere. In this case a 10% error of $\tau_{\text{sun}}^{\text{part}}$=0.1 gives rise to an error of approximately 2% in the aerosol extinction.

The ground based lidar instrumental constant $C_K$ was estimated in the aerosol-free calibration range between 10 to 12 km with constraint on the best match of the $\tau_{\text{KFS}}^{\text{part}}$, $\tau_{\text{TS}}^{\text{part}}$ and $\tau_{\text{sun}}^{\text{part}}$ values by using a calculation chain described in Appendix C.

For 15 May 2004 the best agreement of the $\tau_{\text{KFS}}^{\text{part}}$, $\tau_{\text{TS}}^{\text{part}}$ and $\tau_{\text{sun}}^{\text{part}}$ values was found for a reference value $\beta_{\text{ref}}^{\text{part}}=0.3(\pm0.05)\cdot\beta^{\text{mol}}$ resulting in a lidar constant $C_K=1.65(\pm0.1)\times10^{14}\,\text{mV}\,\text{m}^3\,\text{sr}$. For the same conditions on 19 May 2004 significantly higher value $C_K=2.03(\pm0.1)\times10^{14}\,\text{mV}\,\text{m}^3\,\text{sr}$ was obtained (due to implementation of a new flashlamp in the KARL's hardward and an increase of temperature in the laser room). For the data of 14 April 2005 best agreement was obtained for $\beta_{\text{ref}}^{\text{part}}=0.2(\pm0.05)\cdot\beta^{\text{mol}}$ resulting in a lidar constant $C_K=1.65(\pm0.1)\times10^{14}\,\text{mV}\,\text{m}^3\,\text{sr}$.

With obtained for each day $C_K$ and $\alpha_{\text{TS}}^{\text{part}}(h)$ also the Two-Stream $\beta_{\text{TS}}^{\text{part}}(h)$ profiles were derived directly from Eq. (1). Then the airborne lidar instrumental constant $C_A$ was obtained from Eq. (2). The $C_A=1.43(\pm0.1)\times10^{13}\,\text{mV}\,\text{m}^3\,\text{sr}$ was calculated on 15 May 2004 and 19 May 2004. On 14 Apri 2005 it was $C_A=3.8(\pm0.1)\times10^{13}\,\text{mV}\,\text{m}^3\,\text{sr}$ (due to a setting of 50 V higher PMT voltage).

The Two-Stream $\alpha_{\text{TS}}^{\text{part}}(h)$, $\beta_{\text{TS}}^{\text{part}}(h)$ and $B_{\text{TS}}(h)$ aerosol profiles derived at 532 nm were compared with respective profiles derived using standard method for the Raman KARL's returns. The Raman $\alpha_{\text{RM}}^{\text{part}}(h)$ profiles were derived from the inelastic scattering lidar equation for 607 nm, and Raman $\beta_{\text{RM}}^{\text{part}}(h)$ profiles were calculated from the ratio of 532 nm and 607 nm with mentioned $\beta_{\text{ref}}^{\text{part}}$, for consistency. The Raman evaluation was performed with a 20 min integration in time to assure sufficient SNR and similarily to the Two-Stream case only retrived $\alpha_{\text{RM}}^{\text{part}}(h)$ profiles were smoothed by a running mean



of 300 m.

The Two-Stream profiles (solid lines) and the Raman profiles (dashed lines) for three days under consideration are presented in Figs. 1, 2 and 3.

For 15 May 2004 (Fig. 1) the Two-Stream method was applied to data recorded around 10:00 UT in a height interval between 635 and 2435 m. Two aerosol layers of strongly enhanced particle extinction and lidar ratio, indiscernible in the particle backscatter, are clearly visible in the two-sream as well as in the Raman retrievals. The upper layer with a maximum at 1800 m in the Two-Stream $\alpha_{\text{TS}}^{\text{part}}(h)$ profile has one at a 100 m lower altitude in the Raman $\alpha_{\text{RM}}^{\text{part}}(h)$ profile. The lower layer has a maximum at around 900 m for both retrievals with higher particle extinction values in the Two-Stream profile. The particle optical depth calculated from the Two-Stream interval $\tau_{\text{TS}}^{\text{part}}$ sums up to 0.064, mainly due to contribution from mentioned layers. The sunphotometer particle optical depth $\tau_{\text{sun}}^{\text{part}}$ measured at 10:00 UT in Ny Ålesund was 0.095 for 532 nm. The radiosonde ascent at 11:00 UT in Ny Ålesund confirmed the existence of two inversion layers. One at the altitude of 1200 m characterised by the temperature gradient of $\Delta T_{\text{inv}}=0.014^\circ\text{C}\,\text{m}^{-1}$ and the humidity gradient of $\Delta RH_{\text{inv}}=0.264\%\,\text{m}^{-1}$). The second layer was found at 1800 m with $\Delta T_{\text{inv}}=0.01^\circ\text{C}\,\text{m}^{-1}$ and $\Delta RH_{\text{inv}}=0.525\%\,\text{m}^{-1}$. During this measurement AMAli and KARL recorded volume depolarisation below 5% at 532 nm. The calculations of backward trajectories performed with the NOAA Hysplit Model (Draxler and Rolph, 2003) suggest, that the air remained isolated in the Arctic for at least 6 d. Apart from these two humid layers the air was very clean with particle extinction background values around $1.5\times10^{-5}\,\text{m}^{-1}$ and a lidar ratio around 20 sr, values characterising for the clean Arctic air.

For the 19 May 2004 (Fig. 2) data in a height interval between 815 and 2075 m at around 09:35 UT were analysed. Obtained retrievals coincide well with small deviations only at around 1800 m. Here again a layer of enhanced particle extinction and lidar ratio around 80 sr is visible. On this day even lower values of the particle backscatter were observed. Apart from the layer, the air appears clean, similarly to the previous day.

The $\tau_{TS}^{part}$ was 0.02 and measured at 10:00 UT on that day $\tau_{sun}^{part}$ was 0.11 for 532 nm. Released at 11:00 UT radiosonde recorded a layer at 1800 m with $\Delta T_{inv}$=0.012°C m$^{-1}$ and $\Delta RH_{inv}$=0.14% m$^{-1}$. Both lidars again measured very low volume depolarisation at 532 nm. According to backtrajectories, the air streaked the coastline of north-western Sibiria 3 d prior to its arrival in Ny Ålesund.

On 14 April 2005 (Fig. 3) a height interval between 660 and 2640 m at around 14:45 UT show strongly enhanced $\beta^{part}(h)$, $\alpha^{part}(h)$ and $B(h)$ profiles (if these are compered with both previous days). The lowest values of the particle extinction are around $0.3\times10^{-4}$ m$^{-1}$ corresponding to the maximum of the measured values on 19 May 2004. Likewise, the values of the backscatter are much higher then previously varying between 1–$2.2\times10^{-6}$ m$^{-1}$ sr$^{-1}$. The lidar ratio varies around 34 sr sugesting slightly polluted Arctic atmosphere. The $\tau_{TS}^{part}$ sums up to 0.076 and the sunphotometer measurement at 14:45 UT recorded $\tau_{sun}^{part}$ of 0.084 for 532 nm. At the time corresponding to the evaluation there was no evidence of Cirrus or subvisible clouds in the upper troposphere it in the KARL's signals. Neither KARL nor AMALi recorded significant depolarisation signature at 532 nm. The radiosonde ascent at 12:30 UT recorded a very weak inversion layer at 700 m with $\Delta T_{inv}$=0.005°C m$^{-1}$ and $\Delta RH_{inv}$=0.066% m$^{-1}$, and no evidence of existence of inversions up to the tropopause. The decrease of temperature and relative humidity droping from 50% at 700 m to its minimum of 22% at about 2000 m and rising again to reach 28% at 2500 m shows similarities with the particle extinction profile. The backtrajectories indicated uniform strait transport form the industrial part of Siberia likely for an Arctic Haze event.

### 3.1 Error analysis

The error analysis for the Two-Stream $\alpha_{TS}^{part}(h)$ and $\beta_{TS}^{part}(h)$ profiles was performed according to error propagation. The SNR was determined for each lidar signal $P(h)$ with consideration of a height independent electronic noise $\mu$ and a photon noise for the calculation of a height dependent error $E(h)=\lambda\sqrt{P}(h)+\mu$. The electronic noise $\mu$



was estimated out of the background corrected raw data at the range where no laser light influenced the signals, i.e. for KARL at an altitude interval between 60 and 120 km, and for AMALi in a pretrigger range of 400 m width. The values for $\lambda$ were estimated from altitude intervals with constant aerosol load where variations in the lidar profiles on a scale of individual height increments were assumed to be caused purely by noise, i.e. for KARL in the lower stratosphere and for AMALi in the layers which showed the least height dependent particle contamination in the $\alpha_{TS}^{part}(h)$ and $\beta_{TS}^{part}(h)$ profiles. This caused an overestimation of the noise in the airborne lidar signals when the variability of aerosol in the chosen range interval was present and, hence, a lower limit of the SNR of the airborne lidar was considered.

The molecular extinction and backscatter coefficients $\alpha^{mol}(h)$ and $\beta^{mol}(h)$ necessary for the Rayleigh calibration were calculated from radiosondes profiling. The error in the air density was estimated to be at most 2% for the time difference within two hours with respect to the Two-Stream calculation time. With this assumption approximatlely 10% of the errors in the particle extinction and backscatter coefficients $\alpha^{part}(h)$ and $\beta^{part}(h)$ for both the Two-Stream and Raman approach are caused by possible air density fluctuations.

Errors caused by neglecting the absorbtion due to trace gases and multiple scattering were not concidered.

Figure 4 shows the result of the error analysis for the Two-Stream cases, where the SNR at 532 nm channel for both lidars and the corresponding errors of the Two-Stream $\alpha_{TS}^{part}(h)$ and $\beta_{TS}^{part}(h)$ are given. The higher SNR for the AMALi on 14 April 2005 was caused by higher PMT voltage for the aquisition on that day. The errors of $\alpha_{TS}^{part}(h)$ do not show a pronounced height dependence. In the Two-Stream approach both lidar signals havean opposite gradient of the SNR, which is a clear advantage over evaluation schemes with only one lidar. For the investigated cases the error of the Two-Stream particle extinction is below $\sigma_{ext}^{TS}=2\times10^{-6}$ m$^{-1}$.

Figure 5 gives an estimation of SNR at KARL's 607 nm $N_2$ channel, and errors of the Raman retrived $\alpha_{RM}^{part}(h)$ and $\beta_{RM}^{part}(h)$. As the SNR declines significantly with altitude

the error increases accordingly. In the case of the data presented here, the error of the Raman particle extinction $\sigma_{\text{ext}}^{\text{RM}}$ is almost 10 times higher than the corresponding Two-Stream approach error $\sigma_{\text{ext}}^{\text{TS}}$.

The error of the Two-Stream $\beta_{\text{TS}}^{\text{part}}(h)$ depends almost entirely on the error of the found lidar constants. According to applied constrains the $C_K$ was obtained with 5% insecurity which resulted in an accuracy of the backscatter coefficient below $\sigma_{\text{bsc}}^{\text{TS}}=2\times10^{-7}\,\text{m}^{-1}\,\text{sr}^{-1}$. Any possible errors in the determination of the extinction do not affect the backscatter retrieval. In contrary to the error of $\alpha_{\text{TS}}^{\text{part}}(h)$, the error of $\beta_{\text{TS}}^{\text{part}}(h)$ does not decrease with increasing signal strength. This is due to the fact that the contribution in the error of $\beta_{\text{TS}}^{\text{part}}(h)$ due to an insecurity of the range corrected lidar signal $S$ is proportional to: $\Delta\beta_S \propto \frac{\Delta S}{\sqrt{S}}$. As long as the error in the range corrected lidar signal $\Delta S$ is almost propotional to the root of the signal, there is no dependence on the error of $\beta_{\text{TS}}^{\text{part}}(h)$. The error of the particle backscatter coefficient profiles obtained with in the two-stream and the Raman evaluation are similar for analysed data, as the boundary condition $\beta_{\text{ref}}$, necessary in both cases, determines this insecurity.

A thorough error analysis is recommended then applying the Two-Stream method for another important reason. When two not well matching lidar returns are divided by each other the Two-Stream algorithm can produce a physically unrealistic oscillation in the $\alpha_{\text{TS}}^{\text{part}}(h)$ profile. With simple error analisis this problem can be easily addressed; if an amplitude of the mentioned artificial oscillations exceeds a value expected from the error analysis both employed lidar signals do obviously not contain the same atmospheric signal.

## 4 Discussion

The applicability of the Two-Stream method depends critically on the constraint that both lidars probe into the same air masses. This constraint is often not fulfilled at the



Koldewey Station, where the KARL lidar is installed. It is located near the coastline of Kongsfjord, an area rich in local meteorological phenomenona due to the cliffy orography of Svalbard. Additionally, due to their relative movement AMALi and KARL always detect different air masses directly above the station and below the aircraft. Hence, for the Two-Stream calculations more height steps than required only by a constraint of geometrical compression of each lidar must be excluded. The retrieval is strongly dependent on each lidars' SNR level. The data must be evaluated to obtain as high as possible SNR for as short as possible spatial and temporal averaging. In our case SNR of at least 100 is required (10 min integration time). The optimal configuration for the Two-Stream method employs two lidars with a similar SNR as the particle extinction coefficient retrieval depends on both lidar signals equivalently. To find the most consistent data sets a correlation method was successfully applied.

Obviously the $\tau_{\text{sun}}^{\text{part}}$ obtained from almost simultaneous measurements with a sunphotometer can be compared only roughly with the $\tau_{\text{TS}}^{\text{part}}$ obtained from the Two-Stream particle extinction profiles, due to the short range of the latter retrieval. Care must also be taken while comparing $\tau_{\text{sun}}^{\text{part}}$ with $\tau_{\text{KFS}}^{\text{part}}$ obtained from the standard elastic Klett-Fernald-Sasano inversion applied to KARL' data. The zenith-aiming KARL probed generally different air than the sunphotometer, which measured only at a low elevations above the horizon (about 29° at our polar site). In the direct comparison of the $\tau_{\text{KFS}}^{\text{part}}$ with the $\tau_{\text{sun}}^{\text{part}}$ the latter value can be used only as a rough information. Additionaly, during both campaigns the KARL underestimated signals in the lowermost troposphere (high geometrical compression), which resulted in the underestimation of the $\tau_{\text{KFS}}^{\text{part}}$. Hence, the lidar constant $C_K$, necessary to derive directly the Two-Stream $\beta_{\text{TS}}^{\text{part}}(h)$, was obtained using mainly the constrain of $\tau_{\text{KFS}}^{\text{part}}$ matching the $\tau_{\text{TS}}^{\text{part}}$. At lower latitudes more constraints could have been taken into account, so that an improvement of the retrieval for such cases can be expected.

The Two-Stream $\alpha_{\text{TS}}^{\text{part}}(h)$, $\beta_{\text{TS}}^{\text{part}}(h)$ and $B_{\text{TS}}(h)$ profiles derived from the 532 nm elastic scattering AMALi and KARL signals, were compared with corresponding profiles de-

rived for the KARL's Raman returns. The Raman evaluation was done with a minimum of 20 min integration time to assure sufficient SNR, while the Two-Stream retrievals were obtained with roughly 10 min averages. At the same time the error analysis showed, that the Raman $\alpha^{\text{part}}_{\text{RM}}(h)$ retrievals are obtained with higher errors. Profiles obtained with both techniques (Figs. 1, 2, and 3) agree well, given mentioned insecurities (Figs. 4 and 5) with deviations only in the layers of highest particle extinction values. While for 15 May 2004 one might speculate about a slight height shift between the profiles, such a behaviour is not observed on other days. Therefore, we address these deviations partially to noise, with above given error tolerances, and partially to real variations of the atmosphere during the longer intergration of the Raman-shifted lidar profiles.

For both ASTAR 2004 days lidars recorded mainly clear air with the background particle extinction coefficient around $1.5\times10^{-5}\,\text{m}^{-1}$ and the lidar ratio of 20 sr, i.e. values characteristic for the clean arctic summertime condition. Generaly during ASTAR 2004 campaign, extremely low contaminations were observed (Engvall et al., 2008). The $\tau^{\text{part}}_{\text{sun}}$ averaged for the whole campaign was around 0.08 for the 532 nm, which must be at least partially addressed to the existence of Cirrus and subvisible clouds in the upper troposphere. With both methods humid layers were obtained, which can be characterised by enhanced $\alpha^{\text{part}}(h)$ values, hardly visible in the $\beta^{\text{part}}(h)$ profiles. This once again underlines the necessity to determine backscatter and extinction independently of each other from lidar measurements. The layers retrived on both days at an altitude of about 1800 m (Figs. 1 and 2) match the inversion layers measured by the radiosonde. Although radiosonde launches took place up to two hours after the overflights we assume, that the inversion layers could not be significantly changed during this time period, due to prolonged stable weather conditions on these days (Dörnbrack et al., 2009). The enhanced extinction, together with the high lidar ratios, the high relative humidity and the low volume depolarisation recorded by both instruments on both days suggest that these layers were composed of a very small spherical supercooled water droplets, not unusual in the pristine conditions at the Arctic region (Pinto et al.,



2001; Treffeisen at al., 2007).

Backward trajectories for 15 May 2004 suggest that the air under consideration remained isolated in the Arctic for at least 6 d and no anthropogenic pollutants could be mixed into these aerosol layers. The backtrajectories of 19 May 2004 passed shortly through non-polar regions as the air streaked the coastline of north-western Europe and Sibiria 3 d prior to its arrival in Ny Ålesund. Due to the low extinction of this air, significant particle loads could not be taken up and no anthropogenic pollutants were mixed into it. Therefore, a local origin of such humid layers over the Koldewey Station seems more likely than an advection phenomenon. Nearby mountains with an altitude of around 1000 m cause local meteorological disturbances at the site (Dörnbrack et al., 2009).

On 14 April 2005 a very local source of contaminations with CO, $NO_2$ and $SO_2$ from the coal mining village in Barentsburg on Svalbard was possible. However, the backtrajectories indicate an uniform long-range transport over mid-continental area of Yenisey and Lena Delta where the soot particles can be expected in anthropogenicly contaminater air. This, together with obtained enhanced values of particle extinction and backscatter coefficients accompaning by the slowly varying lidar ratio around 34 sr (significantly higher than value typical for clean Arctic air of around 20 sr), the low humidity verying between 25–35%, and low volume depolarisation (below 10%) indicate occurrence of a weak Arctic Haze event, than a local contaminations.

## 5 Conclusions

The Two-Stream method is an interesting evaluation tool for a combined lidar observations. By means of the Two-Stream algorithm, (i) the two uncalibrated backscatter lidar signals, (ii) the reference backscatter coefficient value at any arbitrary altitude and (iii) the profiles of the molecular extinction and backscatter characterising the Rayleigh atmosphere are enough to retrieve the particle extinction and backscatter coefficient profiles and lidar ratio profile without ambiguity. Unlike for the standard elastic Klett-

Fernals-Sasano inversion algorithm, which affects the gradient of the backscatter profile by wrongly chosen lidar ratio $B(h)$ and $\beta_{\text{ref}}$ value of the scattering at the reference altitude $h_{\text{ref}}$, for the Two-Stream the bad choise of the $\beta_{\text{ref}}$ causes only a bias on the retrieved backscatter profile. If the $\beta_{\text{ref}}$ is not avaliable, the $\beta_{\text{TS}}(h)$ solution can be obtained directly from the lidar equation if at least one of the lidar instrumental constants $C$ is estimated in any aerosol-free layer.

The Two-Stream method turned out to be successful for the inversion of the AMALi and the KARL data at our polar site. The extinction coefficients were retrieved more precisely than with a Raman technique. Acurate retrievals were obtained for both clear and polluted atmospheric conditions. However, in unstable meteorological conditions, the critical constrain is the demand that both instruments probe the very same air to avoid artificial and meaningless extinction values.

In profiles retrived with the Two-Stream and the Raman techniques layers of enhanced values in $\alpha^{\text{part}}(h)$ profiles, indiscernible in the $\beta^{\text{part}}(h)$ profiles, but corresponding to very high $B(h)$ were found in the two cases of the ASTAR campaign. We interpreted them as layers of small spherical water dropplets, of a non-antropogenic and local orography related origin. During the SvalEx campaign case such layers did not appear. Here strongly enhanced profiles of $\alpha^{\text{part}}(h)$ and $\beta^{\text{part}}(h)$ accompaning by almost constant high value of $B(h)$ were interpred as due to the weak Arctic Haze event of long range advection of aged small particles of antropogenic origin from lower latitudes.

The fact that one of the involved instruments in the Two-Stream method must be air/spaceborne and eye-safe makes this approach quite expensive to be used on everyday basis. However, during ASTAR 2007 ample use of this technique to the airborne lidar, ground-based lidar and spaceborne lidar data, especially for the investigations of the late winter's Arctic haze conditions was made. In the future we plan to apply the Two-Stream approach to combined ground based and satellite lidar measurements. In this case in the evaluation scheme more factors will be of a concern, as frequency and time of the satellite overpasses, obtaining sufficient SNR, multiple scattering effects



due to clouds and far range of satellite lidar. An experiment dedicated to the Two-Stream validation and analysis of the CALIPSO satellite nadir-aiming lidar, frequently overflying the Arctic regions, was already performed during various AWI campaigns using zenith-aiming ground based KARL lidar and zenith-aiming airborne AMALi lidar.

## Appendix A

### The Airborne Mobile Aerosol Lidar (AMALi)

The Airborne Mobile Aerosol Lidar (AMALi) is a small portable backscatter lidar designed for remote, simultaneous, high resolution detection of vertical and temporal extent of tropospheric aerosol load and depolarization (Stachlewska et al., 2004, 2009b). In this study the version of the AMALi based on the Nd:Yag laser operating with 15 Hz repetition rate at 1064 nm and 532 nm with pulse energy of 60 mJ and 120 mJ, respectively was used. As a reciever a 10.2 cm parabolic off-axis mirror with FOV of 3.1 mrad was employed. The eye-safety at distances greater than 2.5 km off the system was assured by using a large laser beam divergence of 2.6 mrad. The nadir-aiming airborne measurements were limited to the near range by the eye-safety constrains and the maximum flight altitude of 3 km for the installation onboard a Dornier Do 288 aircraft (the AWI Polar 2 aircraft). Length of retrived profiles varied between 2.5–2.7 km depending on flight altitude and taking into account 235 m losses due to geometrical compression. This limitation allowed to neglect the effects of a multiple scattering possible due to large FOV and large laser beam divergence. For the Two-Stream calculations discussed in this paper the 532 nm signals averaged over 8 min with 60 m range resolution for 90 kt aircraft's speed over ground were used.

## Appendix B

### The Koldewey Aerosol Raman Lidar (KARL)

The Koldewey Aerosol Raman Lidar (KARL) is a ground based system integrated at the Koldewey station in Ny Ålesund, Spitsbergen (78.9° N, 11.9° E) serving for detection of tropospheric aerosols and water vapour (Ritter et al., 2004, 2008). The version of the KARL used for this study employed the Nd:Yag laser operating with 30 Hz repetition rate at 355 nm, 532 nm and 1064 nm, each with energy around 2 W. The recieving system had two mirrors; 10.8 cm diameter with FOV of 2.25 mrad for near range (from 650 m to 6 km) and 30 cm diameter and FOV of 0.83 mrad for far range (from 2 km to lower stratosphere) measurements. Detection was provided at the IR, VIS, UV elastic backscatter channels, VIS depolarisation, and Raman-shifted wavelengths for nitrogen 387 nm and 607 nm and for water vapour 407 nm and 660 nm. For the application to the Two-Stream the 532 nm elastic data with standard averaging over 10 min and 60 m ranging from geometrical compression up to 15 km were used. The inelastic signals at 607 nm were averaged over 20 min and 300 m.

## Appendix C

### Lidar instrumental constants

Usually the lidar instrumental constants are not known precisely. For the standard elastic Klett-Fernald-Sasano and the inelastic Raman-Ansmann evaluation schemes the lidar instrumental constant is redundant (height derivative of height independent variable) and its knowledge is not required. An explicit calculations or measurements of lidar instrumental constant are difficult and suffer from considerable error contributions mainly due to the instabilities of the emitted laser energy, transmission of the optical elements, and the efficiency of the detection (changes in applied voltage and



surrounding temperature).

Th the case of the Two-Stream approach the lidar instrumental constants for the airborne $C_A$ lidar and the ground based $C_K$ lidar can be estimated directly from the Eqs. (1) and (2) if at any height within the Two-Stream application range there is available additional information on $\beta_{\mathrm{ref}}$ (e.g. known for aerosol free range in Tropopause) or the lidar $B(h)$ (e.g. known $B_{\mathrm{Ci}}$ for Cirrus clouds).

When any of the two lidars senses the whole troposphere and the particle optical depth $\tau_{\mathrm{sun}}^{\mathrm{part}}(\lambda)$ is known (performed nearby sunphotometer measurements), the lidar constant of that system, e.g. $C_K$ can be derived by rewriting the Eq. (1) to Eq. (C1). Note that the Eq. (C1) holds only for all heights $h$ in the high troposphere or the tropopause, were the particle extinction coefficient $\alpha^{\mathrm{part}}$ can be neglected and the molecular extinction coefficient $\alpha^{\mathrm{mol}}$ is usualy assumed as known or obtained from performed nearby radiosonde profiling.

$$S_K(h) = C_K \beta(h) \exp\left(-2\tau_{\mathrm{sun}}^{\mathrm{part}}\right) \exp\left(-2\int_0^h \alpha^{\mathrm{mol}} dz\right) \tag{C1}$$

By estimating $\beta(h)$ by $\beta^{\mathrm{mol}}(h)$ derived from the density and temperature profile obtained from the radiosonde the $C_K$ can be obtained as the mean value over all height increments $i$ in the stratosphere (Eq. C2).

$$C_K = \left\langle \frac{S_K(i)}{\beta(i) \exp\left(-2\tau_{\mathrm{sun}}^{\mathrm{part}}\right) \exp\left(-2\int_0^i \alpha^{\mathrm{mol}} dz\right)} \right\rangle_i \tag{C2}$$

The better estimation of the $\beta(h)$ in the free troposphere the more precisely the $C_K$ can be retrieved.

For the purpose of this perticular study the $C_K$ was estimated separately for each of the analysed days. It was estimated in the aerosol-free range between 10–12 km (where $\beta(h) \approx \beta^{\mathrm{mol}}(h)$) by using a standard Klett-Fernals-Sasano elastic inversion of the KARL's data with the following constrains:

– $\tau_{KFS}^{part}$ obtained from Klett-Fernals-Sasano particle extinction profile in the whole range where it was applied should match to the sunphotometer value $\tau_{sun}^{part}$ better than 10%

– $\tau_{KFS}^{part}$ obtained from Klett-Fernals-Sasano particle extinction profile in the range corresponding to the range where the Two-Stream was applied should match to the $\tau_{TS}^{part}(layer)$ obtained from the Two-Stream $\alpha_{TS}^{part}$ better than 5%

– the altitudes where Cirrus or subvisible clouds were detected by KARL at about 9 km were treated with lidar ratio $B_{Ci}$ = 12 (Ansmann et al., 1992)

Note: the underestimated particle extinction from the ground to the KARL's completed geometrical compression at a height $h_{gc}$ was aproximated for all height steps as a constant value equal to the value of the particle extinction obtained with the Two-stream at a height $h_{gc}$ (i.e. $\alpha_{KFS}^{part}(0{:}\Delta h{:}h_{hc}){=}\alpha_{TS}^{part}(h_{gc})$).

For these calculations also an assumption on the lidar ratio was made. Due to the fact that the Arctic atmosphere was relatively clear above the aircraft's flight altitude any reasonably chosen lidar ratio for the remaining altitudes ($10<B<50$) did not significantly alter the standard elastic Klett-Fernald-Sasano solution. Six different profiles for minimal, average and maximal values of the two quantities $\beta_{ref}$ and $B$ (each corresponding to a slightly different value of $C_K$) were obtained. The final value $C_K$ used for the retrieval of the Two-Stream $\beta(h)$ was calculated as a mean averaged over all height positions $i$ in the reference range and over all of the different standard inversion solutions $j$ as in Eq. (C3). From the scattering of $C_K(j)$ around its mean value insecurity of 5% for the determination of the lidar constant was obtained.

$$C_K = \left\langle \left\langle \frac{S_K(i)}{\beta(i)\, T_{[0,i]}^2} \right\rangle_{(i)} \right\rangle_{(j)} \tag{C3}$$

*Acknowledgements.* We acknowledge the NOAA Air Resources Laboratory (ARL) for the provision of the HYSPLIT transport and dispersion model used in this publication.



## References

Ackermann, J.: The extinction to backscatter ratio of tropospheric aerosol: A numerical study, J. Atmos. Ocean. Tech., 15, 1043–1050, 1998. 20231

Ansmann, A., Riebesell, M., and Weitkamp, C.: Measurements of aerosol profiles with Raman lidar, Opt. Lett., 15, 746–748, 1990. 20231

Ansmann, A., Wandinger, U., Riebesell, M., Weitkamp, C., and Michaelis, W.: Independent measurements of extinction and backscatter profiles in cirrus clouds by using a combined Raman elastic-backscatter Lidar, Appl. Opt., 31, 7113–7131, 1992. 20231, 20249

Böckmann, C.: Hybrid regularisation method for ill-posed inversion of multiwavelength lidar data in the retrieval of aerosol size distribution, Appl. Opt., 40, 1329–1341, 2001. 20230

Böckmann, C. and Kirsche, A.: Iterative regularization method for lidar remote sensing, Comput. Phys. Commun., 174(8), 607–615, 2006. 20231

Cuesta, J. and Flamant, P. H.: Two-Stream lidar inversion algorithm for airborne and satellite validations, in: Proceedings of 22nd International Laser Radar Conference (IBC 2004), edited by: Pappalardo, G. and Amodeo, A., ESA SP-561, 1, 471–474, 2004. 20232

Dörnbrack, A., Stachlewska, I. S., Ritter, C., and Neuber, R.: Aerosol distribution around Svalbard during intense easterly winds, Atmos. Chem. Phys. Discuss., 9, 16441–16481, 2009, http://www.atmos-chem-phys-discuss.net/9/16441/2009/. 20243, 20244

Draxler, R. R. and Rolph, G. D.: HYSPLIT (HYbrid Single-Particle Lagrangian Integrated Trajectory) Model, Real-time Environmental Applications and Display sYstem (READY) Website http://www.arl.noaa.gov/ready/hysplit4.html, NOAA Air Resources Laboratory, Silver Spring, MD, 2003. 20238

Engvall, A.-C., Krejci, R., Ström, J., Minikin, A., Treffeisen, R., Stohl, A., and Herber, A.: In-situ airborne observations of the microphysical properties of the Arctic tropospheric aerosol during late spring and summer, Tellus B, 60, 392–404, doi: 10.1111/j.1600.0889.2008.00348.x, 2008. 20243

Fernald, F. G.: Analysis of atmospheric lidar observations: some comments, Appl. Opt., 23, 652–653, 1984. 20231

Klett, J. D.: Stable analytical inversion solution for processing lidar returns, Appl. Opt., 20, 211–220, 1981. 20231

Hughes, H. G. and Paulson, M. R.: Double-ended lidar techniques for aerosol studies, Appl. Opt., 27, 2273–2278, 1988. 20231

Jörgensen, H. E., Mikkelsen, T., Streicher, J., Herrmann, H., Werner, C. and Lyck, E.: Lidar calibration experiments, Appl. Phys. B Lasers O., 64(3), 355–361, 1997. 20231

Klett, J. D.: Lidar inversions with variable backscatter/extinction velues, Appl. Opt., 24, 211–220, 1985. 20231

Kovalev, V. A. and Eichinger, W. E.: Elastic Lidar: Theory, Practice, and Analysis Methods, J. Wiley & Sons, New York, ISBN 0-471-20171-5, 2004. 20233

Kunz, G. J.: Bipath Method as a way to measure the spatial backscatter and extinction coefficients with lidar, Appl. Opt., 26, 794–795, 1987. 20231

Leiterer, U., Weller, M., and Janiak, J.: Verfahren zur Bestrahlungsstärke- und Strahldichtekalibrierung von Spektrometern, Patentschrift DD 228 631 A1, WP GO1 D/265 1067 v. 16.10., 1985. 20236

Müller, D., Wandinger, U., and Ansmann, A.: Microphysical particle parameters from extinction and backscatter data by inversion with regularization, Appl. Opt., 38, 2358–2368, 1999. 20231

Pinto, J. O., Curry, J. A., and Intrieri, J. M.: Cloud-aerosol interactions during autumn over Beaufort Sea, J. Geophys. Res., 106(D14), 15077–15097, 2001. 20243

Pornsawad, P., Böckmann, C., Ritter, C., and Rafler, M.: Ill-posed retrieval of aerosol extinction coefficient profiles from Raman lidar data by regularization, Appl. Opt., 47, 1649–1661, 2008. 20231, 20235

Ritter, C., Kirsche, A., and Neuber, R.: Tropospheric Aerosol Characterized by a Raman Lidar over Spitsbergen, in: Proceedings of 22nd International Laser Radar Conference (ILRC 2004 in Matera, Italy), edited by: Pappalardo, G. and Amodeo, A., ESA SP-561, 1, 459–462, ISBN 92-9092-872-7, 2004. 20247

Ritter, C., Stachlewska, I. S., and Neuber, R.: Application of the Two-Stream evaluation for a case study of Arctic Haze over Spitsbergen, in: Proceedings of 23nd International Laser Radar Conference (ILRC 2006 in Nara, Japan), edited by: Nagasawa, C. and Sugimoto, N., 1, 507–510, ISBN 4-9902916-0-3, 2006. 20232, 20235

Ritter, C., Hoffmann, A., Osterloh, L., and Böckmann, C.: Estimation of the Liquid Water Content of a low-level Arctic winter cloud, in: Proceedings of 24nd International Laser Radar Conference (ILRC 2008 in Boulder, Colorado, USA), 1, 579–582, ISBN 978-0-615-21489-4, 2008. 20247

Sasano, Y., Browell, E. V., and Ismail, S.: Error caused by using a constant extinction/backscattering ratio in the lidar solution, Appl. Opt., 24, 3929–3932, 1985. 20231



Stachlewska, I. S., Wehrle, G., Stein, B., and Neuber, R.: Airborne Mobile Aerosol Lidar for measurements of Arctic aerosols, in: Proceedings of 22nd International Laser Radar Conference (ILRC 2004), edited by: Pappalardo, G., and Amodeo, A., ESA SP-561, 1, 87–89, 2004. 20246

Stachlewska, I. S., Ritter, C., and Neuber, R.: Application of the Two-Stream inversion algorithm for retrieval of extinction, backscatter and lidar ratio for clean and polluted Arctic air, in: Proceedings of SPIE, 5584, 03/1–03/8, 2005. 20231

Stachlewska, I. S., Neuber, R., Lampert, A., Ritter, C., and Wehrle, G.: AMALi the Airborne Mobile Aerosol Lidar for Arctic research, Atmos. Chem. Phys. Discuss., 9, 18745–18792, 2009,
http://www.atmos-chem-phys-discuss.net/9/18745/2009/. 20246

Treffeisen, R., Krejci, R., Ström, J., Engvall, A. C., Herber, A., and Thomason, L.: Humidity observations in the Arctic troposphere over Ny-Ålesund, Svalbard based on 15 years of radiosonde data, Atmos. Chem. Phys., 7, 2721–2732, 2007,
http://www.atmos-chem-phys.net/7/2721/2007/. 20244

Veselovskii, I., Kologotin, A., Griazanow, V., Müller, D., and Whitemann, D.: Inversion with regularization for the retrieval of tropospheric aerosol parameters from multiwavelength lidar sounding, Appl. Opt., 18, 3685–3699, 2002. 20231

Wang, X., Frontoso, M. G., Pisani, G., and Spinelli, N.: Retrieval of atmospheric particles optical properties by combining ground-based and spaceborne lidar elastic scattering profiles, Opt. Express, 15, 6734–6743, 2007. 20232

Winker, D. M., Hunt, B. H., and McGill, M. J.: Initial performance assessment of CALIOP, Geophys. Res. Lett., 34, L19803, doi:10.1029/2007GL030135, 2007. 20232

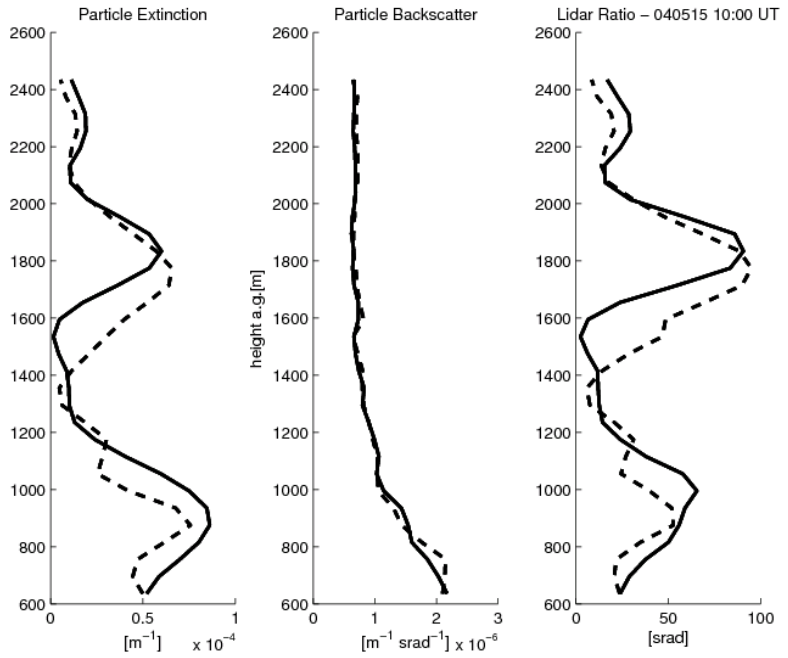


**Fig. 1.** The Two-Stream retrievals (solid) ploted with Raman (dashed) profiles for 532 nm on 15 May during the ASTAR 2004 campaign.



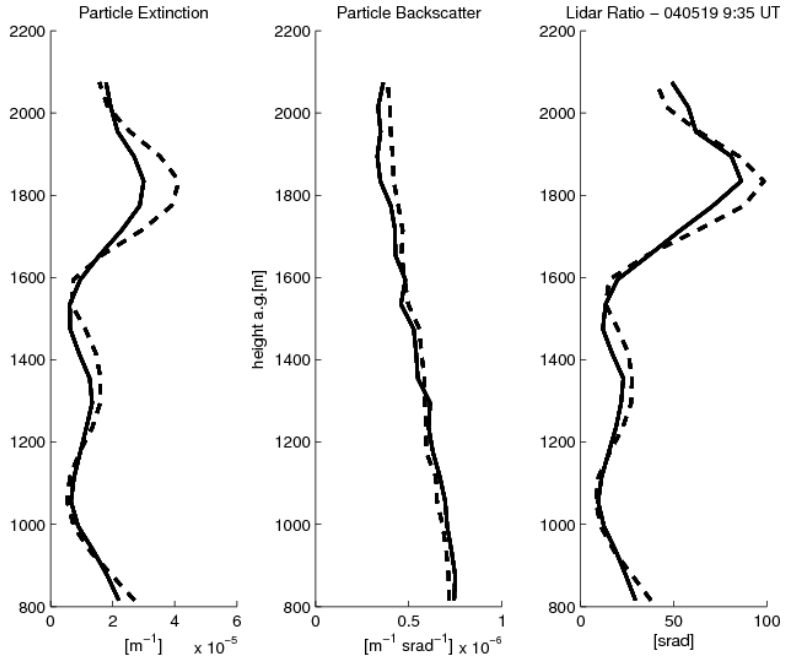


**Fig. 2.** The Two-Stream retrievals (solid) ploted with Raman (dashed) profiles for 532 nm on 19 May during the ASTAR 2004 campaign.

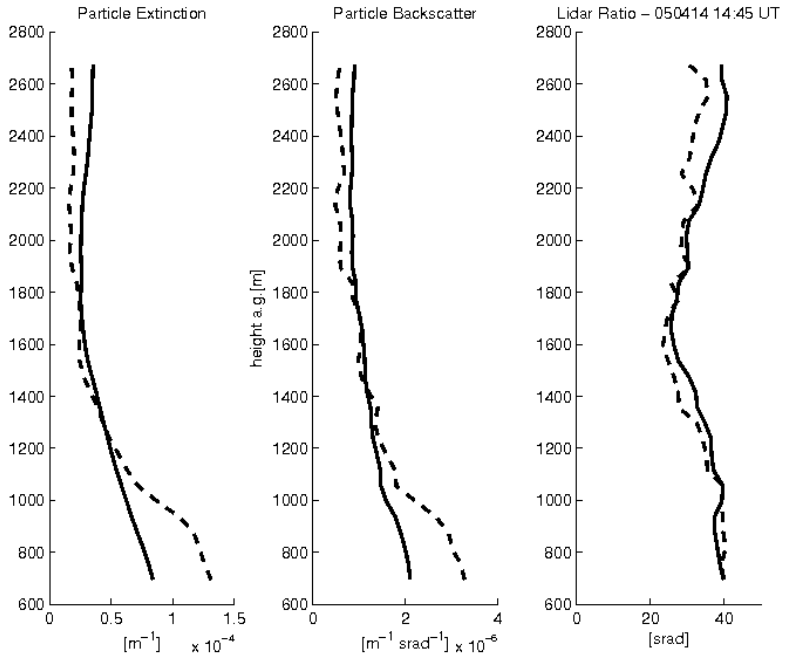


**Fig. 3.** The Two-Stream retrievals (solid) ploted with Raman (dashed) profiles for 532 nm on 14 April during the SvalEx 2005 campaign.



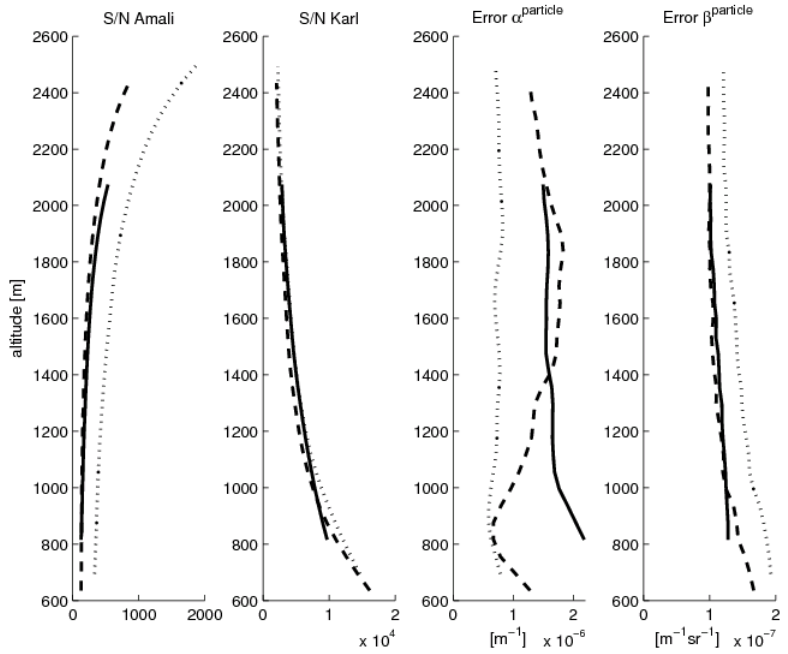


**Fig. 4.** The signal to noise ratio of AMALi and KARL lidars' raw data with the Two-Stream particle extinction and backscatter error values for 15 May 2004 (dashed), 19 May 2004 (solid) and 14 April 2005 (dotted). Values refer to 10 min and 60 m averaging at 532 nm.

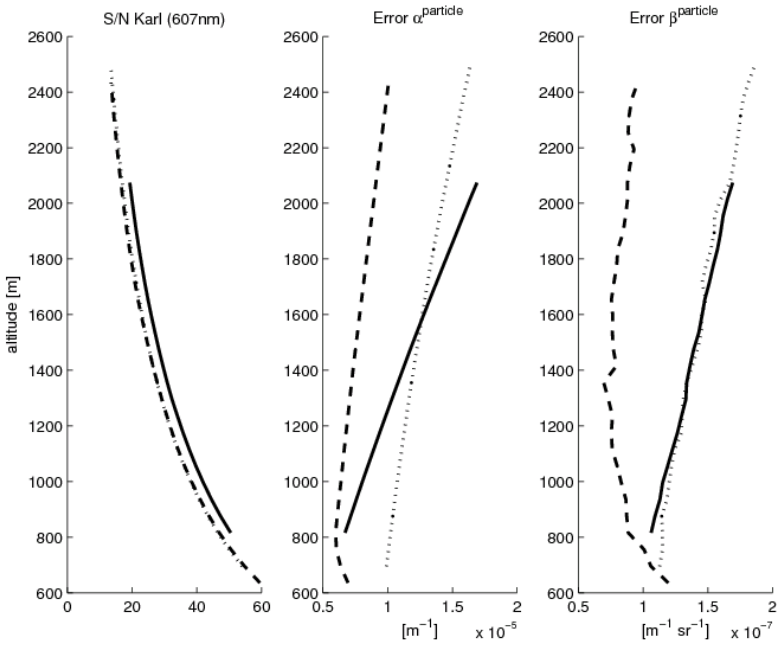


**Fig. 5.** The signal to noise ratio of the KARL's 607 nm $N_2$ Raman channel at 20 min temporal and 60 m spatial averaging. The particle extinction and backscatter error values for 15 May 2004 (dashed), 19 May 2004 (solid) and 14 April 2005 (dotted) according to the standard Raman evaluation method.